



# A new scenario for globular cluster color bimodality and its implication for host galaxy formation

Suk-Jin Yoon

Department of Astronomy, Yonsei University, Republic of Korea  
e-mail: sjyoon@galaxy.yonsei.ac.kr

**Abstract.** In this contribution, I briefly introduce a new scenario for well-known color bimodality found in extragalactic globular cluster (GC) systems and show that it gives a simple, cohesive explanation for the key observations. The implication of the results is discussed in the context of the formation of GC systems and their parent galaxies.

**Key words.** galaxies: star clusters: general — galaxies: formation — galaxies: evolution

## 1. Introduction

Globular clusters (GCs) are among the oldest stellar systems in the observable Universe and are always present in large galaxies. Since GCs form when starbursts occur in galaxies, they carry vital information on the histories of star formation and chemical enrichment of their parent galaxies. Unlike the integrated light from complex stellar populations of galaxies, GCs are easier to interpret thanks to their small internal dispersion in age and abundance. Hence, systematic studies of GC systems are the best means of constraining the formation and evolutionary processes of their host galaxies.

One of the most significant developments in the field of extragalactic GCs over the past couple of decades is the discovery of “bimodal” optical color distributions (e.g.,  $C - T_1$ ,  $V - I$ , and  $g - z$ ) of GC systems. Based on the assumed linear relationship between GC colors and their metallicities, color bimodality

is generally viewed as the presence of merely two GC subsystems with different metallicities within individual galaxies. This notion has formed a critical backbone of various galaxy formation theories.

However, Yoon et al. (2006, 2011a,b, 2013, Kim et al. 2013) proposed a new theory, in which the metallicity-to-color conversion relations are in fact “inflected” and colors trace metallicities in a nonlinear manner. The nonlinear nature of the metallicity-to-color transformation, i.e., the color-metallicity relations, can produce bimodal color distributions from a broad underlying metallicity spread, even if it is unimodal.

## 2. Results

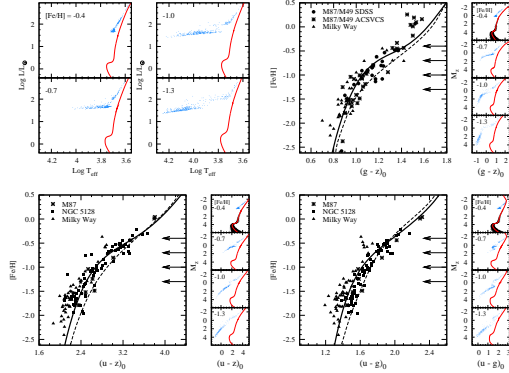
Despite far-reaching implications, whether color-metallicity relations are nonlinear in the form introduced by Yoon et al. (2006), and whether observed GC color bimodalities are caused by the nonlinear relations are under hot debate. On that account, experiments are re-

quired to test the veracity of their theoretical color-metallicity relations and their potential as tools for getting directly GC metallicity distributions from color distributions. The most direct way to do this is by obtaining spectroscopic metallicities for large samples of GCs. Although this is now becoming available for extragalactic GC systems, spectroscopic data of sufficient quality remain observationally expensive, requiring multiple nights of 10 m class telescope time to collect samples of significant sizes.

An alternative, more efficient technique that relies on only using photometric colors was proposed by Yoon et al. (2011a,b, 2013). In essence, this technique uses the fact that if one color distribution (e.g.,  $g - z$ ) has a significantly different “shape” from other color distributions (e.g.,  $u - z$  and  $u - g$ ) for the identical sample of GCs, the assumption that colors are linear proxies of metallicities is invalidated.

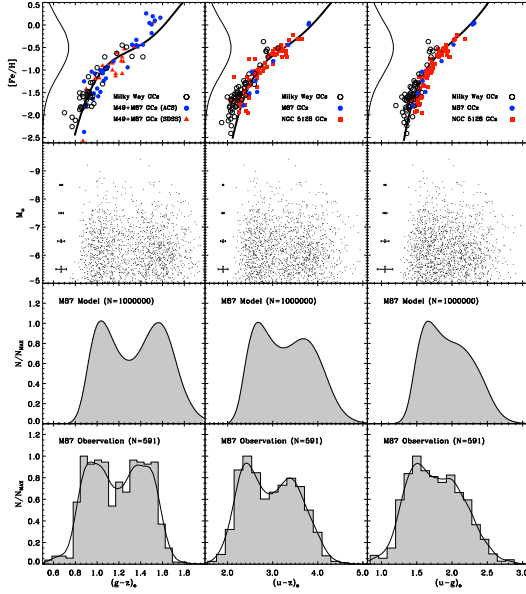
Figure 1 shows the synthetic color-magnitude diagrams for individual stars of the model GCs, and compares the resulting theoretical color-metallicity relations with observations. The stellar population simulations are based on the Yonsei Evolutionary Population Synthesis (YEPS) model (Chung et al. 2013). One of the main assets of our model is the consideration of the systematic variation in the mean color of horizontal-branch stars as functions of metallicity, age, and abundance mixture of stellar populations. It is clear that the color-metallicity relation for the  $u$ -band colors are substantially less wavy than those for the other commonly used broadband colors. This is because the  $u$ -band colors are relatively insensitive to the mean temperature of horizontal-branch stars owing to the Balmer jump where the  $u$ -band is located.

Figure 2 shows multi-band ( $u$ ,  $g$ , and  $z$ ) observation of GCs in M87 and Monte Carlo simulations for their color distributions. M87 is one of the very few early-type galaxies with existing  $u$ -band data. A given metallicity distribution (shown as vertical distributions in the top panels) is projected onto the theoretical color-metallicity relations (shown as solid lines in the upper panel) to create the simulated color distributions in the mid panels. For the set of



**Fig. 1.** Empirical and theoretical color-metallicity relations (CMRs) of GCs, along with synthetic  $\text{Log } T_{\text{eff}} - \text{Log } L/L_{\text{sun}}$  and color-magnitude diagrams of individual stars. (*Upper left quadrant*) Synthetic  $\text{Log } T_{\text{eff}}$  vs.  $\text{Log } L/L_{\text{sun}}$  diagrams of stars for 14-Gyr model GCs with various  $[\text{Fe}/\text{H}]$ 's. Red loci are the Yonsei-Yale ( $Y^2$ ) isochrones depicting main sequence and red giant branch, whereas blue dots represent HB stars based on the  $Y^2$  horizontal-branch (HB) tracts. (*Upper right quadrant*) The observed relationship between  $g - z$  and  $[\text{Fe}/\text{H}]$  for 22 M49 and M87 GCs with SDSS photometry (circles) and 33 M49 and M87 GCs with ACS Virgo Cluster Survey photometry (asterisks), and 40 Galactic GCs with  $E(B - V) < 0.3$  (triangles). The thick solid line is for the 5th-order polynomial fit to our standard model for 14-Gyr GCs (Chung et al. 2013), and the dashed line is for the model without HB stars for comparison. Arrows denote the four values of  $[\text{Fe}/\text{H}]$ , for which the synthetic color-magnitude diagrams are given in the right small panels. The top panel shows individual stars (black and blue dots) with an error simulation, whereas the rest panels show only the corresponding isochrones (red loci) and HB stars (blue dots). (*Lower left quadrant*) Same as the upper right quadrant, but for the  $u - z$  color. (*Lower right quadrant*) Same as the lower left quadrant, but for the  $u - g$  color. (Figure adapted from Yoon et al. 2011a)

colors shown in the figure, the distributions are noticeably different, especially between  $g - z$  and  $u - g$ : while  $g - z$  distribution clearly shows a bimodal case with roughly the same heights for the blue and red peaks, the bimodality in  $u - g$  distribution is substantially diminished with the blue peak now dominating the overall distribution. The observed color distributions



**Fig. 2.** Mutiband ( $u$ ,  $g$ , and  $z$ ) observation of GCs in M87 and Monte Carlo simulations for their color distributions. (*Top row*) Same as the CMRs in Figure 1. The metallicity spread of  $10^6$  model GCs is shown along the y-axis, for which a simple Gaussian distribution is assumed ( $\langle[\text{Fe}/\text{H}]\rangle = -0.5$  dex and  $\sigma([\text{Fe}/\text{H}]) = 0.6$ ). The best-fit age to reproduce the morphologies of  $g-z$ ,  $u-z$ , and  $u-g$  color histograms *simultaneously* is 13.9 Gyr. (*Second row*) The left, middle, and right columns represent the color-magnitude diagrams of 2000 randomly selected model GCs for the  $g-z$ ,  $u-z$ , and  $u-g$  colors, respectively. The colors are transformed from  $[\text{Fe}/\text{H}]$ 's by using the theoretical relation shown in the top row. For the integrated  $u$ -band absolute mag,  $M_u$ , a Gaussian luminosity distribution ( $\langle M_u \rangle = 25.2$ , distance modulus = 31.02, and  $\sigma(M_u) = 1.15$ ) is assumed according to the observation. Observational uncertainties as a function of  $M_u$  shown by error bars are taken into account in the simulations. (*Third row*) The left, middle, and right columns represent the color distributions of  $10^6$  modeled GCs for the  $g-z$ ,  $u-z$ , and  $u-g$  colors, respectively. (*Bottom row*) Same as the third row, but the observed color histograms for the M87 GC system (see Figure 3). The 591 GCs were used that have  $u$ ,  $g$ , and  $z$  measurements in common, and the sample is  $u$ -band limited. Solid lines are smoothed histograms with Gaussian kernels. (Figure adapted from Yoon et al. 2011a)

are remarkably similar to the simulated distri-

butions albeit the slight offsets, thereby confirming that the theoretical color-metallicity relation is justifiable for the case of M87 GC system.

The metallicity-color nonlinearity is also supported strongly by the similar  $u$ -band photometry of M84 GC system (see Yoon et al. 2013 for details) and by spectroscopic absorption index distributions of M31 GCs (see Kim et al. 2013 & Chung et al. 2013 for details).

Hierarchical models of galaxy formation depict the shaping of a single massive galaxy through continuous merging of several thousand small building blocks. This picture of galaxy evolution may leave little room for the possibility of a GC system divided in just two, i.e., metal-rich and metal-poor subpopulations. Our findings challenge the conventional wisdom and greatly simplify theories for formation of GC systems and their host galaxies.

The histories of GCs and their host galaxies are reconstructed as follows. Reader is referred to Yoon et al. (2011b) for the full discussion.

### 1. Giant ellipticals' inner, main haloes:

The inner, main spheroids ( $R \lesssim 1 R_e$ ) of today's giant elliptical galaxies ( $M_B \lesssim -20$ ) were first created in dense regions of the universe via dissipational mergers of a large number of protogalactic gas clouds. The chemical enrichment of the galaxies was rapid, and the difference in the formation epochs of the metal-poor and metal-rich ends of GC metallicity distributions should be small ( $\lesssim 1$  Gyr), as evidenced by observations (e.g., Jordán et al. 2002). In this view, the metal-poor GCs in massive galaxies are the first generation of GCs in the universe.

### 2. Normal ellipticals' entire haloes:

The spheroids (out to  $R \lesssim 10 R_e$ ) of normal (non-giant) galaxies ( $M_B \gtrsim -20$ ) were created later than those of massive ones via self-collapses or mergers of protogalactic clouds that did not take part in giant galaxy formation early on. They were outside of tumultuous, dense regions, and have evolved rather independently from central massive galaxies. This

picture is supported by recent observational evidence that the GC systems in Galactic satellites and some Galactic GCs believed to be accreted from satellite dwarf galaxies are relatively younger than the majority of Milky Way GCs (e.g., Marín-Franch et al. 2009).

### 3. Remote outskirts of giant ellipticals in dense environments:

The remote outer haloes of giant elliptical galaxies have been on the fringes of active, violent gas-rich mergers at the early epochs of galaxy formation, and later experienced dissipationless accretion of stars and GCs from its metal-poor satellite galaxies and/or from the surrounding regions. Such GCs with an accretion origin tend to be of lower metallicity and on highly elongated orbits with high energy. The GCs generally favor the extended outskirts of giant galaxies (Lee et al. 2008; Dirsch et al. 2003), although they, on highly elongated orbits, must penetrate into the inner body of galaxies. This explains the observations that the bimodality in GC colors corresponds to a change in the kinematic properties of the GCs, such that the blue GCs are dynamically hotter and there is a “bimodal” distribution of velocity dispersion. The demarcating radii between the inner, main part (the product of mergers) and the outskirts (the product of

merger plus accretion) are not sharp and vary galaxy-to-galaxy depending on their individual histories of mergers and accretions. This is in line with the considerable diversity in the kinematics of the GC systems in giant elliptical galaxies (e.g., Hwang et al. 2008; Lee et al. 2010).

*Acknowledgements.* I acknowledge support from Mid-career Research Program through the NRF of Korea grant by the MEST (No. 2012R1A2A2A01043870).

### References

- Chung, C., Yoon, S.-J., Lee, S.-Y., & Lee, Y.-W. 2013, *ApJS*, 204, 3  
 Dirsch, B., et al. 2003, *AJ*, 125, 1908  
 Hwang, H. S., et al. 2008, *ApJ*, 674, 869  
 Jordán, A., Côté, P., West, M. J., & Marzke, R. O. 2002, *ApJ*, 576, 113  
 Lee, M. G., et al. 2008, *ApJ*, 682, 135  
 Lee, M. G., et al. *ApJ*, 709, 1083  
 Marín-Franch, A., et al. 2009, *ApJ*, 694, 1498  
 Kim, S., et al. 2013, *ApJ*, *submitted*  
 Yoon, S.-J., Yi, S. K., & Lee, Y.-W. 2006, *Science*, 311, 1129  
 Yoon, S.-J., et al. 2011a, *ApJ*, 743, 149  
 Yoon, S.-J., et al. 2011b, *ApJ*, 743, 150  
 Yoon, S.-J., et al. 2013, *ApJ*, *submitted*